Atmos. Chem. Phys. Discuss., https://doi.org/10.5194/acp-2017-505
Manuscript under review for journal Atmos. Chem. Phys.
Discussion started: 6 June 2017

Atmospheric Chemistry and Physics Discussions

Particulate trimethylamine in the summertime Canadian high Arctic lower troposphere

Franziska Köllner[1,2], Johannes Schneider[1], Megan D. Willis[3], Thomas Klimach[1], Frank Helleis[1], Heiko Bozem[2], Daniel Kunkel[2], Peter Hoor[2], Julia Burkart[3], W. Richard Leaitch[4], Amir A. Aliabadi[4,a], Jonathan P.D. Abbatt[3], Andreas B. Herber[5], and Stephan Borrmann[1,2]

[1]Max Planck Institute for Chemistry, Mainz, Germany
[2]Institute for Atmospheric Physics, Johannes Gutenberg University Mainz, Germany
[3]Department of Chemistry, University of Toronto, Canada
[4]Environment Canada, Toronto, Canada
[5]Alfred Wegener Institute for Polar and Marine Research, Bremerhaven, Germany
[a]now at: Environmental Engineering Program, University of Guelph, Guelph, Canada

Correspondence to: Franziska Köllner (f.koellner@mpic.de)

Abstract. Size-resolved and vertical profile measurements of single particle chemical composition (sampling altitude range 50 - 3000 m) were conducted in July 2014 in the Canadian high Arctic during the aircraft-based measurement campaign NETCARE 2014. We deployed the single particle laser ablation aerosol mass spectrometer ALABAMA (vacuum aerodynamic diameter range approximately 200 - 1000 nm) to identify different particle types and their mixing states. On basis of the single particle analysis, we found that a significant fraction (23 %) of all analyzed particles (in total: 7412) contained trimethylamine (TMA). The identification of TMA in ambient mass spectra was confirmed by laboratory measurements. From the maximum occurrence of particulate TMA in the Arctic boundary layer and the higher abundance of smaller TMA-containing particles (maximum in the size distribution at 300 nm), we conclude that the TMA component of these particles resulted from emissions within the Arctic boundary layer. Air mass history according to FLEXPART backward simulations and associated wind data give evidence of a marine-biogenic influence on particulate TMA. The marine influence on particle chemical composition in the summertime Arctic is further demonstrated by the existence of larger sodium and chloride ("Na/Cl-") containing particles which are mainly abundant in the boundary layer. Some of these sea spray particles were internally mixed with carbohydrates (e.g., cellulose) which likely originated from a sea surface microlayer enriched with microorganisms and organic compounds. The external mix of sea spray particles and TMA-containing particles suggests the latter result from secondary conversion of precursor gases from marine inner-Arctic sources. In contrast to TMA- and Na/Cl-containing aerosol types, particles with biomass-burning markers (such as levoglucosan) showed a higher fraction at higher altitudes, thereby indicating long-range transport as their source. Our measurements highlight the importance of natural, marine inner-Arctic sources for summertime Arctic aerosol.

Atmos. Chem. Phys. Discuss., https://doi.org/10.5194/acp-2017-505
Manuscript under review for journal Atmos. Chem. Phys.
Discussion started: 6 June 2017

1 Introduction

A remarkable increase in Arctic near-surface air temperature (e.g., Chapman and Walsh, 1993; Serreze et al., 2009) has led to rather drastic changes of several climate parameters, in particular a decreasing sea ice extent of 3.5 % to 4.1 % per decade since 1979 (IPCC, 2014, with further evidence up to 2017 from the National Snow and Ice Data Center, Boulder, Colorado, https://nsidc.org). Among the processes driving Arctic warming aerosol particles play a key role due to their direct and indirect radiative effects. The impact of aerosol particles on the radiation budget strongly depends on number concentration, size and chemical composition (e.g., Haywood and Boucher, 2000). Different measurements at Arctic sites show a strong annual cycle in these aerosol characteristics (e.g., Tunved et al., 2013; Leaitch et al., 2013). Three main processes drive the annual cycle in Arctic aerosol. First, a smaller polar dome surface extent in summer leads to reduced pollution sources within the Arctic. Second, efficient wet removal processes in liquid clouds leading to a smaller condensation sink in the summertime Arctic. Third, the substantial change in duration of daylight in Arctic summer leads to increased photochemical processes and/or increased biological activity, which further result in a higher nucleation potential. (e.g., Law and Stohl, 2007; Quinn et al., 2007; Schmale et al., 2011; Rahn and McCaffrey, 1980; Barrie, 1986; Stohl, 2006; Engvall et al., 2008; Kupiszewski et al., 2013; Heintzenberg et al., 2017; Croft et al., 2016a; Burkart et al., 2017; Kawamura et al., 1996, 2010).

To better understand the physical and chemical processes leading to a higher nucleation potential and a frequent appearance of clouds in the summertime Arctic, it is crucial to study emissions of the terrestrial and oceanic biosphere. So far, a few studies have discussed the importance of methanesulfonic acid (MSA), an oxidation product of dimethylsulfide emitted from ocean biomass, to take part in aerosol chemistry in the Arctic (e.g., Croft et al., 2016b; Leaitch et al., 2013; Sharma et al., 2012; Willis et al., 2016; Mungall et al., 2016). It is further known that marine biota also release certain gas-phase amines, such as trimethylamine (TMA), into the atmosphere (e.g., Ge et al., 2011a; Van Neste et al., 1987; Gibb et al., 1999; Facchini et al., 2008) which subsequently may contribute to aerosol chemistry. Numerous chamber, modeling and field studies at southern latitudes (e.g., Almeida et al., 2013; You et al., 2014; Bergman et al., 2015; Müller et al., 2009) have focused on sources, emission rates and gas-to-particle partitioning processes of atmospheric amines. So far, this research has shown that amines may take part in aerosol chemistry in several ways. These include acid-base reactions to form aminium salts and dissolution in cloud droplets (owing to their high water-solubility) where subsequent acid-base reactions can occur in the aqueous phase (e.g., Glasoe et al., 2015; Dawson et al., 2012; Erupe et al., 2011; Ge et al., 2011b; Jen et al., 2016, 2014; Youn et al., 2015; Yu et al., 2012; Rehbein et al., 2011; Pankow, 2015). Amines compete with ammonia (NH_3) in neutralizing acidic aerosol. Which base is favored by these reactions depends on several parameters, such as acidity of the aerosol, Henry's law coefficient and the concentration of both substances in the atmosphere (e.g., Pratt et al., 2009; Barsanti et al., 2009). Amines further may take part in aerosol chemistry via gas-phase oxidation processes leading to the formation of species such as amides, nitramines and imines. Resulting lower volatility products can go on to form secondary organic aerosol (SOA) (e.g., Murphy et al., 2007; Ge et al., 2011b; Angelino et al., 2001).

Despite these considerable advances in studies of atmospheric amines, very little is known about their abundance in Arctic regions. Scalabrin et al. (2012) reported marine influence on amino acids in Arctic aerosol. Further particle measurements at

Mace Head, Ireland have shown the presence of organic compounds, such as amines, in aerosol that originated in polar marine air masses (Dall'Osto et al., 2012). However, our knowledge about the influence of amines on Arctic aerosol number concentration, size and chemical composition remains incomplete. Based on a study of Almeida et al. (2013), Leaitch et al. (2013) and Croft et al. (2016b) speculated about the contribution of amines to particle nucleation in the Arctic. Amines can further essentially contribute to condensational growth of summertime Arctic aerosol particles.

For this reason the main objective of this research is to investigate emission sources and aerosol chemistry processes of particulate TMA in the summertime Arctic. We used aircraft-based single particle chemical composition measurements conducted in the Arctic summer. In addition, we analyze concurrent data from further aerosol and trace gas instruments as well as Lagrangian modeling simulations by FLEXPART. This study provides an important opportunity to advance our understanding of the strong biological control over the summertime Arctic aerosol.

2 Experimental and modeling section

2.1 Description of the sampling site and measurement platform

As one part of the NETCARE project (Network on Climate and Aerosols: Addressing Key Uncertainties in Remote Canadian Environments), aircraft-based measurements were deployed from Resolute Bay, Nunavut (Canada) during 4 - 21 July 2014. In this study, we focus on measurements made during 4 - 12 July 2014. During this time, six research flights (around 20 flight hours) were performed. Flight tracks covered altitudes from 50 to 3000 m above continental as well as marine (partly covered with sea ice) regions (Fig. 1). The satellite image from 4 July 2014 shown in Fig. 1 presents sea ice and open water conditions around Resolute Bay, which can be regarded as typical during 4 - 12 July. Three flights aimed to sample above two polynyas north of Resolute Bay. Notably, the sea ice south-east of Resolute Bay and close to the ice edge in Lancaster Sound was largely covered with melt ponds.

The instrument platform was the research aircraft Polar 6, a modified Basler BT-67 maintained by Kenn Borek and operated by the Alfred Wegener Institute for Polar and Marine Research (Herber et al., 2008). The aircraft was equipped with instruments to measure meteorological state parameters, several trace gases as well as aerosol particle number, size and chemical composition. In general, aerosol instruments were connected to a forward-facing near-isokinetic stainless steel inlet, which was followed by a 1 inch-stainless steel manifold inside the cabin. All instruments were connected to the common inlet line system with 1/4-inch stainless steel tubing. Reactive trace gases were measured via a second PTFA inlet line. Further detailed information on the inlet and sampling strategy can be found in Leaitch et al. (2016), Willis et al. (2016), Burkart et al. (2017) and Aliabadi et al. (2016b).

Atmos. Chem. Phys. Discuss., https://doi.org/10.5194/acp-2017-505
Manuscript under review for journal Atmos. Chem. Phys.
Discussion started: 6 June 2017

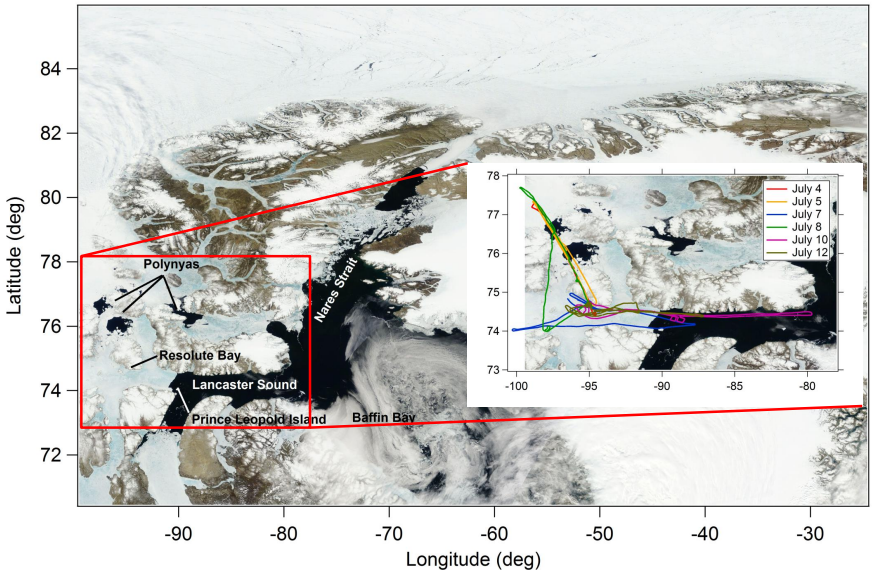

Figure 1. Satellite image (visible range from MODIS) from 4 July 2014 showing sea ice and open water conditions around Resolute Bay, in Lancaster Sound, Nares Strait and Baffin Bay. The inset shows a compilation of flight tracks conducted during 4 - 12 July 2014 (indicated with different colors). Image are courtesy of NASA Worldview: https://worldview.earthdata.nasa.gov.

2.2 Instrumentation

The following section provides a brief description of the instrumentation that is relevant to this discussion.

Number concentrations of particles greater than 5 nm in diameter ($N_{d>5nm}$) were measured with a TSI 3787 water-based ultrafine condensation particle counter (UCPC). Particle size distributions of particles greater than 250 nm ($N_{d>250nm}$) were measured using an optical particle counter from GRIMM (model 1.129 Sky-OPC). Measurements of carbon monoxide (CO) were conducted with an Aerolaser ultra-fast CO monitor (model AL 5002). State parameters and meteorological measurements were made using an AIMMS-20 from Aventech Research Inc. Detailled information on measurement principles and instrument calibrations are given in Leaitch et al. (2016), Aliabadi et al. (2016b) and Bozem et al. (2017), in prep.

In order to provide information about the chemical composition of single aerosol particles, the ablation aerosol mass spectrometer ALABAMA (Aircraft-based Laser Ablation Aerosol Mass Spectrometer; Brands et al. (2011)) was deployed on the Polar 6 during NETCARE 2014. The basic measurement principle of the ALABAMA is as follows: first, the particles enter the system through a pressure-controlled inlet (PCI). While ambient pressure changes, this device (custom-made at the Max Planck Institute for Chemistry) maintains a constant pressure in the following aerodynamic lens by varying the volume flow rate into the instrument. A flexible orifice is either squeezed or relaxed, depending on atmospheric pressure, by a bottom and

top plate which are connected to a rotor (Molleker et al. (2017), in prep.). After passing through the PCI, particles are focused into a narrow beam with the help of a Liu-type aerodynamic lens (Liu et al., 1995a, b). The focused particles are detected by two light scattering signals (using 405 nm laserdiodes and photo-multipliers) allowing the determination of the size-dependent particle velocity. By comparing these values with the velocity of manufactured monodisperse polystyrene latex (PSL) particles in different sizes, we can derive the particle vacuum aerodynamic diameter (d_{va}). Next, the particles enter the ablation and ionization region in the high-vacuum system. The particles are ablated and ionized by a single triggered laser shot (266 nm, frequency-quadrupled Nd:YAG laser). In the final step, cations and anions produced by laser ablation are guided into a bipolar Z-ToF (Z-shaped Time of Flight) mass spectrometer, which provides bipolar mass spectra. Due to limitations of the aerodynamic lens transmission efficiency and the lower detection limit of the photo-multipliers, the ALABAMA covers a particle size range from approximately 200 to 1000 nm.

2.3 FLEXPART- Lagrangian particle dispersion model

FLEXPART (FLEXible PARTicle dispersion model (here: version 10.0 beta)) is a Lagrangian particle dispersion model (e.g., Stohl et al., 2005). For our analysis, we used operational analysis data from the European Centre for Medium-Range Weather Forecast (ECMWF) with 0.125° spatial and three hour time resolution. FLEXPART was operated in backward mode to provide potential emission sensitivity (PES) maps. We used PES maps together with sea ice and open ocean coverage derived from the satellite image in Fig. 1 to determine the total residence time of the measured air mass above open water regions three days prior to sampling in altitudes up to 340 m. The model output frequency was set up to one hour and 0.125° spatial resolution.

2.4 Single particle spectra analysis

Particle mass spectra collected by the ALABAMA are analyzed using the software package CRISP (Concise Retrieval of Information from Single Particles) which includes m/z (mass to ion charge ratio) calibration of bipolar mass spectra, peak area integration and analysis of mass spectra using marker peaks for different substances (Klimach, 2012).

The marker method requires knowledge of certain marker peaks in the spectrum belonging to a certain substance and a certain marker threshold (ion peak area threshold). The typical fragmentation pattern of a substance due to laser ablation is crucial for defining the distinct marker peaks. Fragmentation depends on laser wavelength and energy. Marker peaks of many substances are already well-known from laboratory measurements with the ALABAMA (Schmidt et al., 2017) and additionally from literature of other single particle mass spectrometers using the same ablation laser wavelength. Table 1 lists marker peaks of substances used in this study to identify the external and internal mixing state of particles. In addition to the listed references, we performed further laboratory measurements with the ALABAMA in order to identify the fragmentation pattern of TMA-containing particles (Sect. 2.5).

To decide whether a signal is present, we used an ion peak area threshold of 10 mV, respectively 25 mV for positive and negative mass spectra. Both thresholds are chosen as a conservative measure on the basis of the signal intensities of the non-occupied m/z values. A detailed explanation on this topic can be found in the Supplement S1.

Atmos. Chem. Phys. Discuss., https://doi.org/10.5194/acp-2017-505
Manuscript under review for journal Atmos. Chem. Phys.
Discussion started: 6 June 2017

Table 1. Chemical classes and their acronyms used in this study. Associated marker peaks and the compilation of different marker peaks due to fragmentation of the particle ("Marker conditions"), additional comments and used references are given.

Chemical class (Acronym)	Marker conditions	Comments	References
Trimethylamine (TMA)	m/z +59 ($(CH_3)_3N^+$); +58 ($C_3H_8N^+$)	Additionally examined in laboratory measurements with ALABAMA (Sect. 2.5)	(1), (2), (3), (4)
Sodium and chloride (Na/Cl)	m/z +23 (Na^+); (at least two of the following ions) +46 ($Na_2{}^+$), +62 (NaO^+), +63 ($NaOH^+$); (at least two of the following ions) +81/+83 (Na_2Cl^+), -35/-37 (Cl^-), -93/-95 ($NaCl_2{}^-$)	Indicator for sea spray particles Isobaric interference with MSA at m/z -95	(1), (5), (6), (7)
Elemental carbon (EC)	(at least six of the following ions) m/z +36, +48, +60, ..., +144 ($C_{3-12}{}^+$) and/or (at least six of the following ions) m/z -36, -48, -60, ..., -144 ($C_{3-12}{}^-$)	Except m/z -96 ($C_8{}^-$) due to the isobaric interference with $SO_4{}^-$	(7)
Carbohydrates (e.g., levoglucosan, cellulose)	(at least two of the following ions) m/z -45 ($CHO_2{}^-$), -59 ($C_2H_3O_2{}^-$), -71 ($C_3H_3O_2{}^-$)/ 73 ($C_6H^-/C_3H_5O_2{}^-$)	Levogluosan as indicator for biomass burning particles	(8), (9), (10), (11), (12)
Potassium (K)	m/z +39 (K^+)		(1), (7), (13)
Ammonium (NH_4)	m/z +18 ($NH_4{}^+$)		(1), (7), (13)
Methanesulfonic acid (MSA)	m/z -95 ($CH_3O_3S^-$)	Isobaric interference with $PO_4{}^-$ can be excluded due to missing ion signal for $PO_3{}^-$ at m/z -79	(14)
Sulfate (S)	(at least one of the following ions) m/z -97 ($HSO_4{}^-$), -96 ($SO_4{}^-$)		(1), (7)

The semicolon (;) serve as "and". Given reference numbers are defined as follows: (1)Roth et al. (2016); (2)Angelino et al. (2001); (3)Healy et al. (2015) (4)Rehbein et al. (2011); (5)Sierau et al. (2014); (6)O'Dowd and de Leeuw (2007) ; (7)Schmidt et al. (2017); (8)Silva et al. (1999); (9)Corbin et al. (2012); (10)Simoneit (2002); (11)Simoneit et al. (1999); (12)Lakshmanan et al. (1969); (13)Brands et al. (2011); (14)Gaston et al. (2010).

Atmos. Chem. Phys. Discuss., https://doi.org/10.5194/acp-2017-505
Manuscript under review for journal Atmos. Chem. Phys.
Discussion started: 6 June 2017

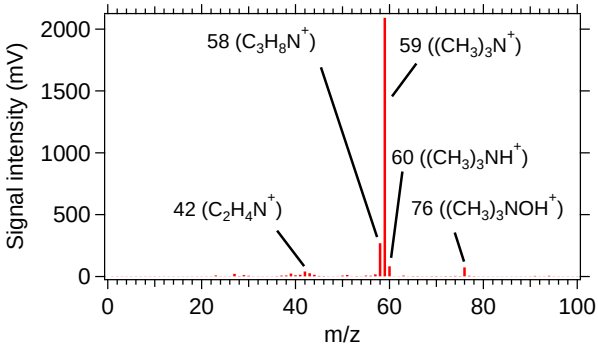

Figure 2. Mean cation spectrum of 88 single particle spectra analyzed within the TMA laboratory measurements.

2.5 Laboratory measurements of TMA-containing particles

In order to identify specific marker peaks of TMA, we conducted laboratory measurements. A mixture of TMA dissolved in water, additional milli-q water and sulfuric acid was nebulized with an aerosol generator (PALAS model AGK2000). Afterwards, these droplets passed through a diffusion dryer filled with silica gel to remove water. The particles were size selected with a Differential Mobility Analyzer (TSI model 3080) (set to 300 nm) and then guided into the ALABAMA and an optical particle counter (GRIMM model 1.129). The energy of the ablation laser was around 1 mJ/pulse. The ablation laser energy deployed during the NETCARE 2014 campaign was between 3 and 4 mJ/pulse. However, we expect no significant differences regarding marker peaks for TMA.

As can be seen in Fig. 2, the most common fragmentation pattern shows peaks at m/z +59 ($(CH_3)_3N$) (molecular ion of TMA) and m/z +58 (C_3H_8N). These measurements confirm previous observations with the ALABAMA (Roth et al., 2016) and with other single particle mass spectrometers using the same wavelength (e.g., Angelino et al., 2001; Healy et al., 2015; Rehbein et al., 2011). Further ion signals at m/z +60 and m/z +76 could be explained by protonation and oxidation of TMA (Angelino et al., 2001).

Despite the addition of sulfuric acid, negative ion mass spectra show poor signals (not shown here). Potential reasons are discussed in the Supplement S2.

3 Results and Discussions

3.1 Meteorological conditions during the NETCARE 2014 campaign

The measurement period from 4 - 12 July 2014 was characterized by generally clear skies, calm wind speeds (Fig. 3) and occasional scattered to broken stratocumulus clouds (Leaitch et al., 2016) due to a high pressure system prevailing around Resolute Bay. Based on low CO mixing ratios, low aerosol number concentrations (Fig. 3) and backward trajectory analysis (Bozem et al., 2017, in prep), air masses measured in this period experienced a weak mid-latitudinal influence and were mainly

Atmos. Chem. Phys. Discuss., https://doi.org/10.5194/acp-2017-505
Manuscript under review for journal Atmos. Chem. Phys.
Discussion started: 6 June 2017

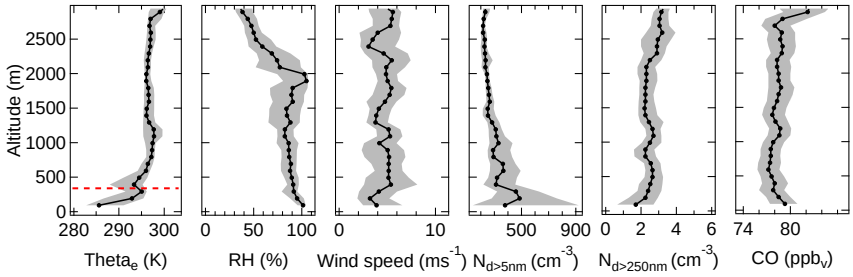

Figure 3. Vertically resolved median (black line) and interquartile ranges (grey shaded area) of the equivalent potential temperature (Theta$_e$), relative humidity (RH), wind speed, particle number concentration measured by the UCPC ($N_{d>5nm}$) and Sky-OPC ($N_{d>250nm}$) as well as CO mixing ratio (including all conducted flights from 4 - 12 July 2014). Measurements of $N_{d>250nm}$ started on 8 July due to prior technical issues. The red line depicts the derived mean upper height of the boundary layer during this measurement period (approximately 340m).

affected by local emission sources (also denoted as "Arctic air mass period" in Burkart et al. (2017)).

As shown in Fig. 1, our measurements took place largely over remote areas, which are dominated by Arctic vegetation, open water regions (e.g., polynyas, Lancaster Sound) and sea ice coverage. Furthermore, seabird colonies were located close to the ice edge in Lancaster Sound and are likely a source of ammonia (Wentworth et al., 2016). Anthropogenic emissions might have affected our measurements, but are mainly related to the sparse Arctic settlements (Aliabadi et al., 2015) and can be ruled out by comparison with other tracers (e.g., CO). We can therefore expect that our observations were mainly influenced by biogenic emissions (in particular marine-biogenic emissions) during this measurement period.

As evident from vertical profiles of equivalent potential temperature (Theta$_e$) (Fig. 3), the mean upper boundary layer (BL) height for this measurement period was at around 340 $\pm$ 100 m. The vertical resolution of the profile in Fig. 3 (100 m) justifies the range of the mean BL height. The mean BL height within its range can be confirmed by results from an extensive study on BL height, mixing and stability during the NETCARE 2014 campaign (Aliabadi et al., 2016a). The capping temperature inversion above 390 m, inferred from values of Theta$_e$, represents a transport barrier for air masses between the BL and the free troposphere (FT). The BL, compared to the FT, was characterized by lower wind speeds, higher relative humidity (RH) and enhanced particle number concentration $N_{d>5nm}$ in contrast to $N_{d>250nm}$, indicating an enhanced number of ultrafine particles due to nucleation in the Arctic BL. A detailed discussion on this topic is given in Burkart et al. (2017).

3.2 Size- and vertically resolved aerosol composition

In total, 7412 particles were analyzed by the ALABAMA during the first phase of this measurement campaign (4 - 12 July 2014), whereby 6970 particle spectra included size information. Applying the marker method (Sect. 2.4), we obtained four distinct particle types. According to the chemical composition, we classified the particles as TMA-, Na/Cl-, EC- and levoglucosan-containing particles. TMA- and levoglucosan-containing particles, with relative fractions of 23 % and 20 %, respectively, appear to be the most prominent particle types. Only 2 % and, respectively, 1 % of all analyzed particles are assigned as EC-

Atmos. Chem. Phys. Discuss., https://doi.org/10.5194/acp-2017-505
Manuscript under review for journal Atmos. Chem. Phys.
Discussion started: 6 June 2017

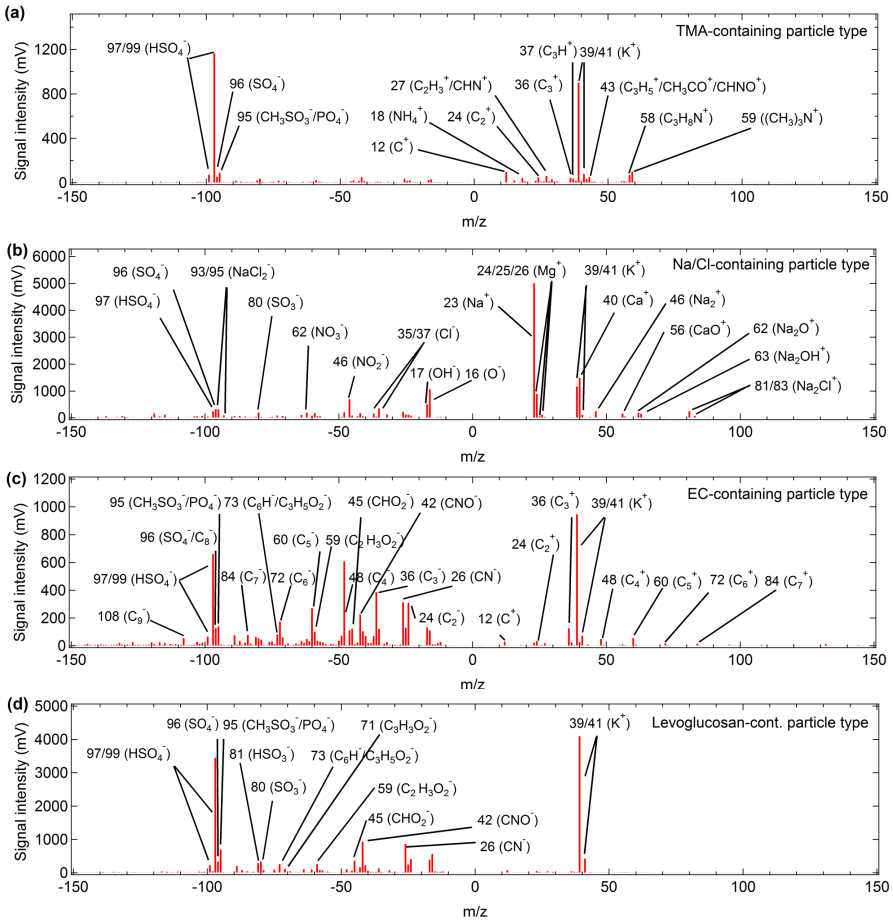

Figure 4. Bipolar mean spectrum of 1688 (23 %) TMA-containing single particle spectra (a), 106 (1 %) Na/Cl-containing single particle spectra (b), 138 (2 %) EC-containing single particle spectra (c) and 1517 (20 %) levoglucosan-containing single particle spectra (d).

and Na/Cl-containing particles. The mean spectra in Fig. 4 combined with the listed additional ion signals in Tab. 2 give an overview of the average chemical composition of each particle type.

In order to describe the unique characteristics of TMA-containing particles compared to other particle groups, Fig. 5 and 6 depict the size and vertical distribution, respectively, of each particle type. Both figures show the fractional abundance of each particle type per size bin, respectively, per altitude bin. We show relative numbers of particles in order to eliminate the size-dependent transmission and detection efficiency of the ALABAMA (Fig. 5) and the sampling time dependence on particle number at different altitudes (Fig. 6).

Atmos. Chem. Phys. Discuss., https://doi.org/10.5194/acp-2017-505
Manuscript under review for journal Atmos. Chem. Phys.
Discussion started: 6 June 2017

Table 2. Overview of the obtained four particle types and their internal mixing state (chemical composition) derived from the mean spectra in Fig. 4 and 7. Signals for sulfate (m/z -97/99 (HSO_4^-), -96 (SO_4^-)) and potassium (m/z +39/41 (K^+)) were present in every mean spectra and have therefore not been listed here.

Particle type denotation	Characteristic ion signals in mean spectrum	Additional ion signals in mean spectrum	Corresponding chemical composition
TMA-containing	m/z +59 ($N(CH_3)_3^+$), +58 ($NC_3H_8^+$)		TMA
		m/z +18 (NH_4^+), C_{1-3}^+, +27 ($C_2H_3^+/CHN^+$), +37 (C_3H^+), +43 ($C_3H_5^+/CH_3CO^+/CHNO^+$)	ammonium, carbon cluster ions, hydrocarbons, oxidized organics, MSA
		m/z -95 ($CH_3O_3S^-$)	
Na/Cl-containing	m/z +23 (Na^+), +46 (Na_2^+), +62 (NaO^+), +63 ($NaOH^+$), +81/+83 (Na_2Cl^+) m/z -35/-37 (Cl^-), -93/-95 ($NaCl_2^-$)		sodium, chloride
		m/z +24/25/26 (Mg^+), +40 (Ca^+), +56 (CaO^+)	magnesium, calcium,
		m/z -45 (CHO_2^-), -59 ($C_2H_3O_2^-$), -71 ($C_3H_3O_2^-$)/ 73 ($C_6H^-/C_3H_5O_2^-$), -46 (NO_2^-), -62 (NO_3^-)	carbohydrates (e.g., cellulose), nitrate
EC-containing	C_{1-7}^+, C_{1-8}^-		carbon cluster ions
		m/z -26 (CN^-), -42 (CNO^-), -45 (CHO_2^-), -59 ($C_2H_3O_2^-$), -73 ($C_6H^-/C_3H_5O_2^-$), -95 ($CH_3O_3S^-$)	cyanide, levoglucosan, MSA
Levoglucosan-containing	m/z -45 (CHO_2^-), -59 ($C_2H_3O_2^-$), -71 ($C_3H_3O_2^-$)/ 73 ($C_6H^-/C_3H_5O_2^-$)		levoglucosan
		m/z -26 (CN^-), -42 (CNO^-), -95 ($CH_3O_3S^-$)	cyanide, MSA

3.2.1 Levoglucosan- and EC-containing particle types

Both levoglucosan and EC-containing particle types are known to be primarily produced from fossil fuel and biomass combustion processes (e.g., Bond et al., 2007; Andreae and Merlet, 2001; Simoneit et al., 1999; Simoneit, 2002). In particular, levoglucosan is formed via the breakdown of cellulose during biomass burning processes. Internal mixing with sulfate and MSA (Fig. 4c,d and Tab. 2) indicates that those particles were exposed to condensational growth with sulfuric and methane-

Atmos. Chem. Phys. Discuss., https://doi.org/10.5194/acp-2017-505
Manuscript under review for journal Atmos. Chem. Phys.
Discussion started: 6 June 2017

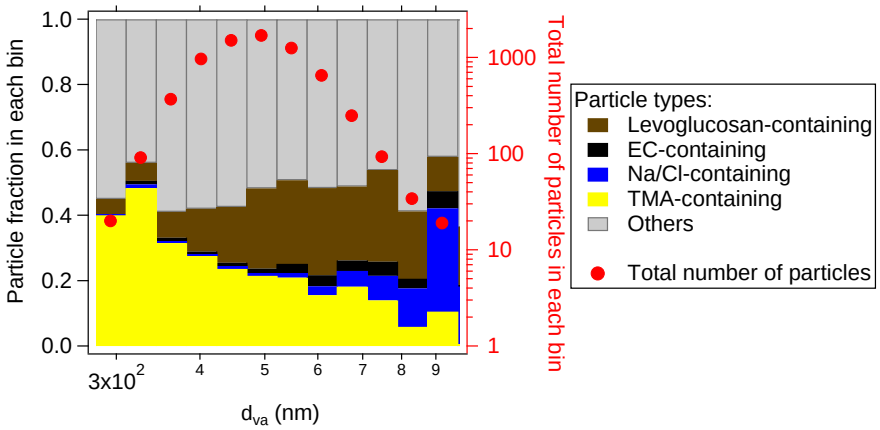

Figure 5. Cumulative size-resolved aerosol composition of the particle types analyzed by the ALABAMA: TMA-containing (yellow), Na/Cl-containing (blue), EC-containing (black), levoglucosan-containing (brown) particles. The number of particles analyzed by the ALABAMA per size bin is shown with red dots.

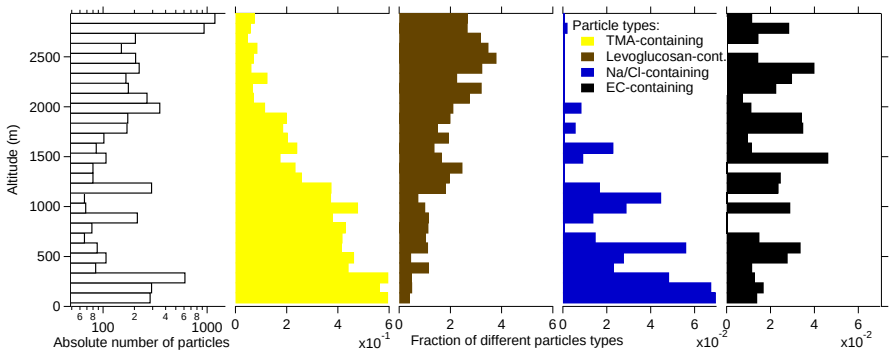

Figure 6. Vertically resolved aerosol composition of the main four particle types analyzed by the ALABAMA: Absolute number of particles analyzed by the ALABAMA (white), TMA-containing (yellow), levoglucosan-containing (brown), Na/Cl-containing (blue) and EC-containing (black) particles. There are in general two levels (below 340 m and above 2700 m) with enhanced number of particles analyzed by the ALABAMA which is caused by a longer sampling time within these altitudes.

sulfonic acid. This may be consistent with observations of their particle size distribution shifted towards larger sizes with maximum diameter at around 700 to 800 nm (Fig. 5). Furthermore, the concurrent presence of cyanide on particulate levoglucosan (Fig. 4d and Tab. 2) confirms the biomass burning source (e.g., Li et al., 2000). From the vertical profiles given in Fig. 6, it can be seen that the fraction of levoglucosan-containing particles increases with increasing altitude, whereas the profile of EC-containing particles shows no vertical dependence. For the levoglucosan-containing particles, the vertical profile corresponds slightly to enhanced CO mixing ratios and $N_{d>250nm}$ (Fig. 3) suggesting a connection to polluted air masses.

Atmos. Chem. Phys. Discuss., https://doi.org/10.5194/acp-2017-505
Manuscript under review for journal Atmos. Chem. Phys.
Discussion started: 6 June 2017

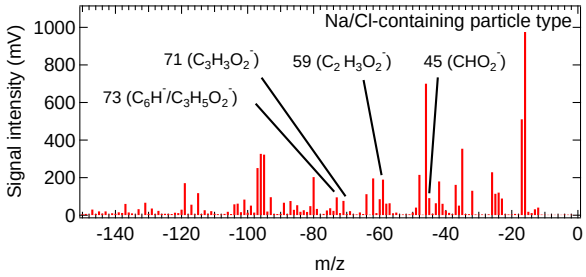

Figure 7. Expanded mean anion spectrum of 106 (1 %) Na/Cl-containing single particle spectra from Fig. 4b. Only the organics peaks are highlighted here.

Taken together, enhanced signals at higher altitudes of levoglucosan, $N_{d>250nm}$ and CO likely originate from long-range transport of polluted air masses.

3.2.2 Na/Cl-containing particle type

A number of studies have reported on the primary production of sea spray particles via bubble bursting at the sea surface (e.g., Blanchard and Woodcock, 1980; O'Dowd and de Leeuw, 2007). Na/Cl-containing particles observed in this study show particle diameters mainly larger than 600 nm and they primarily exist at lowest altitudes which indicates that we also measured locally emitted sea spray particles. The occurrence of sulfate and nitrate ion signals in the mean spectrum (Fig. 4b and Tab. 2) suggests that some particles have already been exposed to chemical aging via reactions with sulfuric and nitric acid forming nitrate and sulfate and releasing HCl in the gas phase (e.g., Sorensen et al., 2005; O'Dowd et al., 1999; Sierau et al., 2014). Moreover, Na/Cl-containing particles are internally mixed with magnesium and calcium, a finding that has recently been reported also by Salter et al. (2016). A further internal mixing of Na/Cl-containing particles with MSA cannot be finally ruled out since $NaCl_2$ and MSA have an isobaric interference at m/z -95 (Tab. 1). However, due to the concurrent existence of other Na and Cl ion signals as well as signals at m/z -93 (isotope of $NaCl_2$), it is likely that ion signals at m/z -95 are largely produced by $NaCl_2$. Interestingly, approximately 50 % of the Na/Cl-containing spectra show ion signal peaks at m/z -45, -59 and -71/-73 (Fig. 7) indicating the concurrent existence of carbohydrates such as cellulose. Previous studies have already reported the occurrence of organic-rich sea spray particles originating from microorganisms and organic compounds enriched in the sea surface microlayer and their importance for cloud formation especially in remote regions (e.g., Quinn et al., 2014; Hawkins and Russell, 2010; Frossard et al., 2014; Wilson et al., 2015; Blanchard and Woodcock, 1980).

3.2.3 TMA-containing particle type

In contrast to the other particle types, the size distribution of TMA-containing particles is shifted towards much smaller diameters (Fig. 5) and the fractional abundance is increasing with decreasing altitude (Fig. 6). Figure 8, a size and vertically resolved profile of particulate TMA, further illustrates that particles detected at the lowest altitudes are smaller compared to particles

Atmos. Chem. Phys. Discuss., https://doi.org/10.5194/acp-2017-505
Manuscript under review for journal Atmos. Chem. Phys.
Discussion started: 6 June 2017

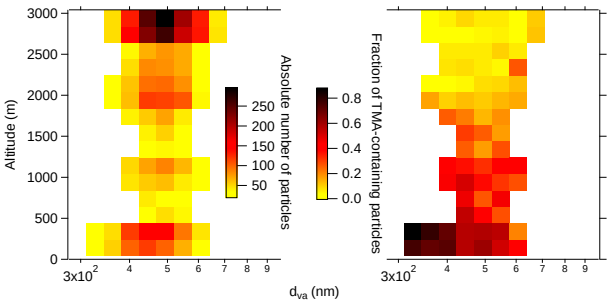

Figure 8. Size- and vertically resolved profile of the absolute number of particles analyzed by the ALABAMA (left, color-coded) and the fraction of TMA-containing particles (right, color-coded). For statistical reasons, the vertical bin size is 200 m. Grid cells with less than 20 particles in total are not considered.

aloft, indicating the presence of younger aerosol particles at lower levels. According to these results together with the existence of a stable stratified BL (Fig. 3), we can infer that those particles originate from inner-Arctic sources.

Possible inner-Arctic sources of TMA, referring to Ge et al. (2011a), are given by oceanic phytoplankton biomass (or other marine organisms) and various human activities (e.g., waste incineration, vehicle exhaust, residential heating). As was pointed out in the introduction to this paper, gaseous TMA emissions may then take part in aerosol chemistry in several ways including acid-base reactions, oxidation processes, dissolution in cloud droplets and nucleation (e.g., Ge et al., 2011a, b; Murphy et al., 2007; Angelino et al., 2001; Rehbein et al., 2011; Erupe et al., 2011).

The mean spectrum of TMA-containing particles (Fig. 4a) shows no indications that further N-containing compounds (such as amine oxidation products, e.g., amides, nitramines and imines) than TMA with the specific ion signals at m/z +59 and +58 were present on the particles. This result suggests that oxidation of TMA did not take part in the formation of particulate TMA. Figure 4a and Table 2 further illustrate the internal mixing of sulfate and TMA which indicates that aminium sulfate salts may be present (e.g., Murphy et al., 2007; Barsanti et al., 2009; Smith et al., 2010). We can therefore hypothesize that the formation of particulate TMA was accompanied with acid-base reactions including TMA, sulfuric and methanesulfonic acid and/or sulfate (e.g., Facchini et al., 2008). It is further possible, due to the occasional presence of low-level clouds (Leaitch et al., 2016), that the formation of TMA-containing particles was favored by the presence of pre-existing wet and acidic particles. Rehbein et al. (2011) reported enhanced gas-to-particle partitioning of TMA by dissolution in cloud/fog droplets and subsequent formation of aminium salts.

3.3 Internal mixing state of TMA-containing particles

The internal mixing state of TMA-containing particles was further analyzed by applying the marker method introduced in Sect. 2.4 for compounds which are apparent in the mean spectrum (Fig. 4a and Tab. 2), such as potassium (K), ammonium (NH_4), MSA and sulfate .

The diagram in Fig. 9 illustrates the classification algorithm as follows: the upper branch always refers to a positive re-

Atmos. Chem. Phys. Discuss., https://doi.org/10.5194/acp-2017-505
Manuscript under review for journal Atmos. Chem. Phys.
Discussion started: 6 June 2017

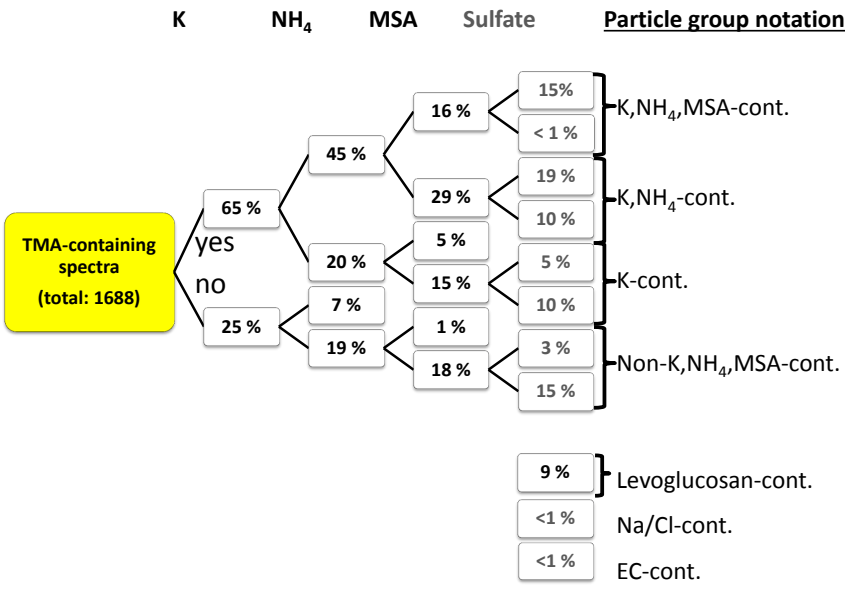

Figure 9. Classification of TMA-containing particles on basis of their different internal mixing states. Each branch describes the existence or non-existence of several substances (potassium (K), ammonium (NH_4), MSA and sulfate) on TMA-containing particles with relative abundances normalized to the occurrence of 1688 TMA-containing particles. Based on this classification four TMA-containing particle sub-types arise "K,NH_4,MSA-cont.","K,NH_4-cont.","K-cont." and "Non-K,NH_4,MSA-cont." as noted behind the braces. We further considered an internal mixing of all TMA-containing particles with levoglucosan (9 %), Na/Cl and EC, whereby the latter two types with relative fractions of less than 1 % are negligible for the further analysis.

sponse ("yes") for whether different marker ion signals are present in spectra or not; the lower branch shows the opposite answer ("no"). Besides the substances which already appeared in the mean spectrum of TMA-containing particles, here TMA-containing spectra are also marked on the concurrent existence of levoglucosan, Na/Cl and EC. The particle sub-group notation is based on the existing or non-existing substances in TMA-containing particles. We do not consider in detail the concurrent existence of carbon cluster ions (m/z +12, +24, ..), different hydrocarbons (m/z +27 and +37) and oxidized organics (m/z +43) since 90 % of all TMA-containing particles contain at least one of these ion signals. For reasons of clarity, particle types with equal and less than 7 % fractional abundance (correspond to a total number of 118 particles) are not explicitly considered in the further analysis, but summarized to "Others".

Following the categorization in Fig. 9, 13 groups of different internal mixing states arise. Notably, in total around 35 % of all TMA-containing spectra do not include sulfate. Moreover, in most cases, when ions with m/z -97 and/or m/z -96 are missing (below ion peak threshold of 25 mV, Sect. 2.4), the negative mass spectrum generally shows no anion signals. Reasons for missing anion signals are further discussed in Supplement S2. Briefly summarized, we cannot definitively determine whether

Atmos. Chem. Phys. Discuss., https://doi.org/10.5194/acp-2017-505
Manuscript under review for journal Atmos. Chem. Phys.
Discussion started: 6 June 2017

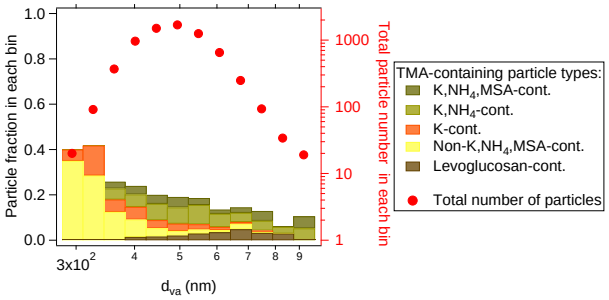

Figure 10. Cumulative size-resolved aerosol composition of the five TMA-containing particle sub-types (normalized to all particles analyzed by the ALABAMA): "K,NH_4,MSA-containing" (dark green), "K,NH_4-containing" (light green), "K-containing" (orange), "Non-K,NH_4,MSA-containing" (yellow) and "levoglucosan-containing" (brown) particles. The number of particles analyzed by the ALABAMA per size bin is shown with red dots.

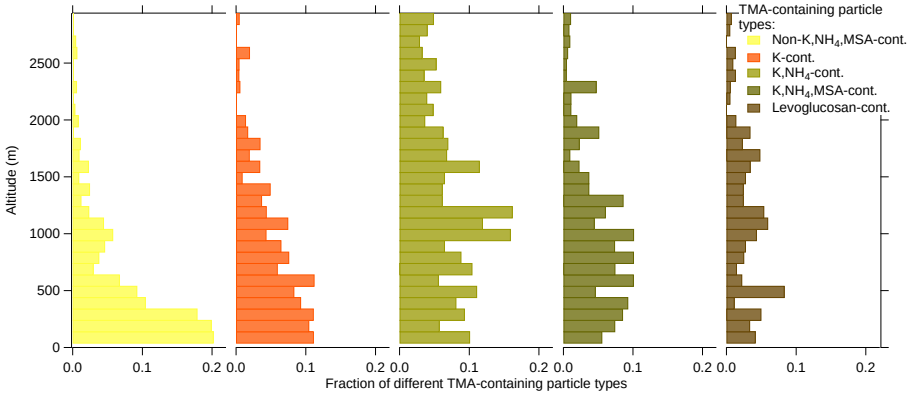

Figure 11. Vertically resolved aerosol composition of the five TMA-containing particle sub-types: "K,NH_4,MSA-containing" (dark green), "K,NH_4-containing" (light green), "K-containing" (orange), "Non-K,NH_4,MSA-containing" (yellow) and "levoglucosan-containing" (brown) particles.

the missing anion signal (and thereby the sulfate signal) is real or caused by other factors such as higher RH values (Neubauer et al., 1998). The TMA-containing particle sub-groups and their denotations are therefore independent on the presence of sulfate. Taken together, five TMA-containing particle sub-types (given with braces in Fig. 9) are considered for further analysis: "K,NH_4,MSA-", " K,NH_4-" "K-", "Non-K,KNH_4,MSA"- and "levoglucosan-containing" particles.

A large fraction (25 %, Fig. 9) of particulate TMA is neither internally mixed with potassium nor with any other primary particulate matter. Earlier studies reported potassium particles to be primary in origin and emitted from biomass burning and other biogenic sources (e.g., Andreae, 1983; Li et al., 2003; Pöhlker et al., 2012). From the absence of any primary component in these particles, we can infer that these TMA-containing particles resulted from SOA formation. In particular, spectra of the TMA-containing particle sub-type "Non-K,NH_4,MSA-containing" (18 %, Fig. 9) show ion signals only for sulfate and

fragments of hydrocarbons (not shown here). The associated particle size distribution (Fig. 10) demonstrates that these particles are mainly present in a size range between 280 and 380 nm. These findings suggest that this TMA sub-type experienced less condensational growth and coagulation in comparison with other sub-types. Furthermore, "Non-K,NH_4,MSA-containing" particles are most abundant at lowest levels (Fig. 11), which further supports the hypothesis that gaseous TMA is emitted from inner-Arctic sources.

Further, 74 % of TMA-containing particles are additionally composed of primary components potassium (Fig. 9, 65 %) and levoglucosan (Fig. 9, 9 %). According to Pöhlker et al. (2012), this internal mixture can be explained by potassium-containing particles acting as seeds for the condensation of different organic material. Thus, the measured particulate TMA can be considered as a secondary component on pre-existing primary particles. The main abundance of these particles at sizes larger than 400 nm, in contrast to "Non-K,NH_4,MSA-containing" particles, further confirms this conclusion. Moreover, the presence of potassium in a single particle spectrum must be interpreted with caution since laser ablation single particle aerosol spectrometers are rather sensitive to this compound due to the very low ionization energy of potassium.

Approximately 39 % of the measured particulate TMA is not internally mixed with ammonium (Fig. 9) but partly with MSA and/or sulfate indicating the presence aminium salts. It shows that amines, beside ammonia, may take part in the neutralization of acidic aerosol. This is of particular interest considering the reduced sources of ammonia in the Arctic and the ocean as a net sink of NH_3 in the summertime Canadian Arctic (Wentworth et al., 2016).

Thus far, our analysis of the size and vertical distribution as well as the internal mixing state of TMA-containing particles indicates the presence of secondary particulate TMA in the Arctic BL, whereby gaseous TMA is emitted from inner-Arctic sources. However, the abundance of TMA-containing particles above the local BL (mainly the sub-types of "K,NH_4,MSA-containing", "K,NH_4-containing", "K-containing" and "levoglucosan-containing", Fig. 11) may be explained by transport of air masses aloft to our measurement site.

3.4 Source apportionment analysis of TMA-containing particles

This section will explore potential emission sources of TMA in the Arctic BL. Thus, the further analysis was restricted to measurements below 340 m (mean upper BL height, Sect. 3.1).

Figure 12 shows the temporal distribution of "non-TMA-containing" particles, such as Na/Cl-, EC- and levoglucosan-containing particles and all TMA-containing sub-types. Figure 13 depicts the spatially resolved fraction of TMA-containing particles below 340 m (left panel) as well as the measured wind direction (right panel) for measurements on 4, 7 and 8 July. We further used three-day FLEXPART backward simulations (Sect. 2.3) for air mass history analysis of the respective three measurement legs (Fig. 14).

Potential emission sensitivity maps combined with sea ice coverage (Fig. 1) show that air masses measured on 4 and 7 July spent less than one hour and around seven hours, respectively, in the last three days in regions of open water (polynyas north of Resolute Bay and Nares Strait). On both days the air was mainly advected above sea ice and snow covered regions north of Resolute Bay (Fig. 14 compared with Fig. 1). The prevailing wind direction on 4 and 7 July along the flight tracks (Fig. 13) is from the north and east and therefore consistent with FLEXPART backward simulations (Fig. 14). From measurements on 4

Atmos. Chem. Phys. Discuss., https://doi.org/10.5194/acp-2017-505
Manuscript under review for journal Atmos. Chem. Phys.
Discussion started: 6 June 2017

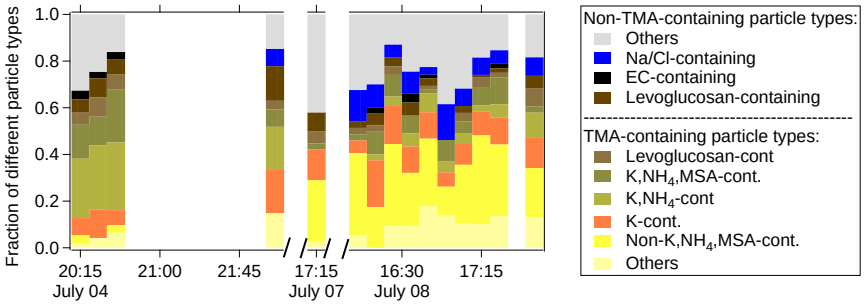

Figure 12. Temporally resolved aerosol composition of Na/Cl-cont. (blue), EC-cont. (black) and levoglucosan-cont. (brown) particle types and "Others" (grey) as well as all TMA-containing particle sub-groups ("levoglucosan-containing" (light brown), "K,NH_4,MSA-containing" (dark green), "K,NH_4-containing" (light green), "K-containing" (orange), "Non-K,NH_4,MSA-containing" (yellow) particle types and "Others" (light yellow)). Fractional abundances of the particle types were calculated for 10 minutes time intervals. Only time intervals with a total number of measured particles larger than 20 were considered. Measurements inside the BL on 5, 10 and 12 July did not provide any 10-min time interval with more than 20 spectra.

and 7 July it is not possible to attribute TMA emissions to marine-biogenic or anthropogenic (e.g., vehicle exhaust, residential heating and waste incineration emissions in Resolute Bay) sources, therefore a more detailed air mass history analysis was done with the data of 8 July.

On 8 July the prevailing wind direction along the presented flight leg is from the east (Fig. 13) with wind speeds up to 5 m/s (not shown here). The fraction of TMA-containing particles decreases with a shift to a more southerly wind direction (yellow to green colors, Fig. 13) and the highest fractional abundance of particulate TMA was measured close to the ice edge (Fig. 13) at low wind speeds close to 0 m/s. We can therefore hypothesize that air masses with enhanced fraction of particulate TMA measured during this flight segment were influenced by marine-biogenic emissions, which is further supported by an increased fractional abundance of Na/Cl-containing particles on 8 July (Fig. 12). This inference is confirmed by the analysis of air mass history with three-day FLEXPART backward simulations (Fig. 14) for the presented flight leg in Fig. 12. The PES map illustrates that these air masses were mainly marine influenced from Lancaster Sound and Baffin Bay regions and partly from open water regions in Nares Strait (compare with Fig. 1). Air masses measured during the considered flight leg on 8 July resided for more than 17 hours during the three days prior to sampling above regions of open water. With regard to the measured low CO values, anthropogenic influences on gaseous amine emissions from Resolute Bay are negligible. It is further conceivable that the ice edge in the western section of Lancaster Sound where the highest surface phytoplankton production rate and chlorophyll *a* concentration were measured (M. Gosselin, personal communication) and/or large bird colonies at Prince Leopold Island (Fig. 1) (Wentworth et al., 2016) contribute to TMA emissions into the atmosphere. Previous aerosol chemical composition measurements on Bird Island in the South Atlantic (> 50°S) have already shown the presence of amines and amino acids emitted from local fauna including seabirds, penguins and fur seals (Schmale et al., 2013).

Another important finding is that primary sea spray particles (Na/Cl-containing) and TMA-containing particles measured on 8

Atmos. Chem. Phys. Discuss., https://doi.org/10.5194/acp-2017-505
Manuscript under review for journal Atmos. Chem. Phys.
Discussion started: 6 June 2017

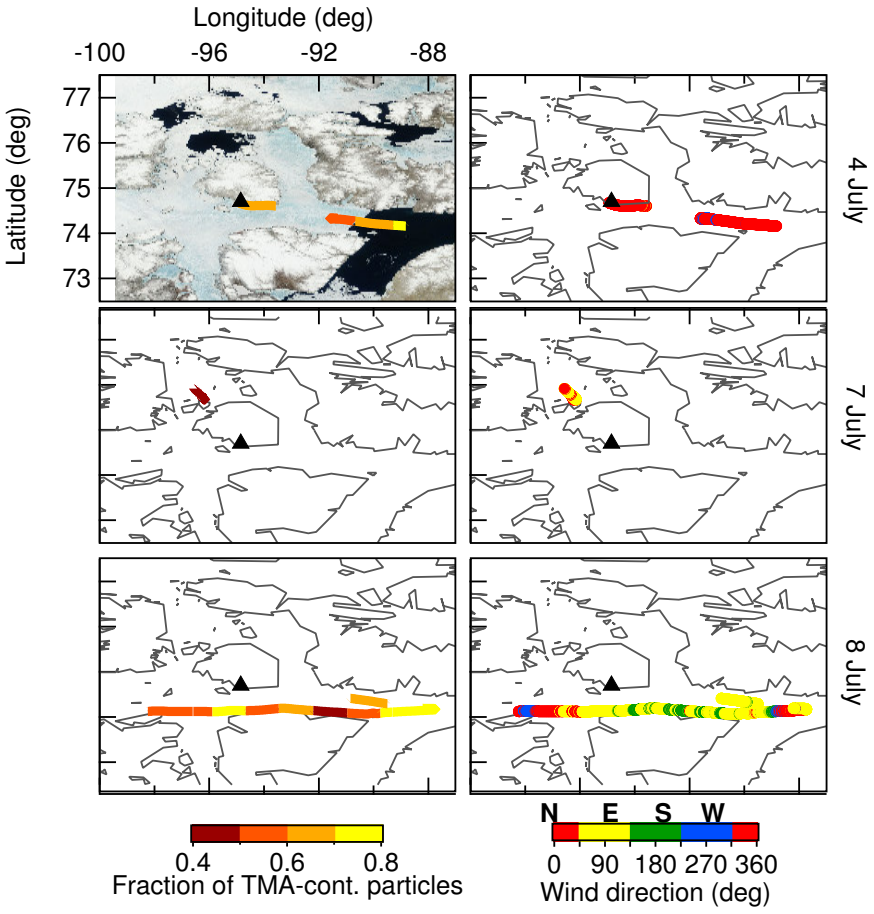

Figure 13. Spatially resolved fraction of TMA-containing particles (left column, color-coded) and wind direction (right column, color-coded) below 340 m. Different rows present different measurement days. The first graph additionally shows the satellite image on 4 July in the visible range. Further satellite images are not presented here due to negligible changes in sea ice coverage from 4 - 8 July. Abbreviations N, E, S and W refer to North, East, South and West. The black triangle presents the location of Resolute Bay on the map.

July are externally mixed (Fig. 12) although both substances seems to be released from the ocean. This analysis solidifies the earlier hypothesis (Sect. 3.3) that particulate TMA presents secondary aerosol (Facchini et al., 2008). The higher abundance of the TMA-containing particle sub-type "Non-K,NH_4,MSA-containing" on 8 July (Fig. 12) further supports the conclusion of SOA formation.

It is further relevant to discuss that on 8 July from 15:50 UTC until 17:20 UTC (respective flight leg in Fig. 12) we flew low over sea ice in the vicinity of dissipating low-level clouds. These clouds had formed above the open water regions east of our flight leg (Burkart et al., 2017; Leaitch et al., 2016). We can therefore assume that cloud processing likely contributed to enhanced gas-to-particle partitioning of TMA as earlier reported in Rehbein et al. (2011).

Atmos. Chem. Phys. Discuss., https://doi.org/10.5194/acp-2017-505
Manuscript under review for journal Atmos. Chem. Phys.
Discussion started: 6 June 2017

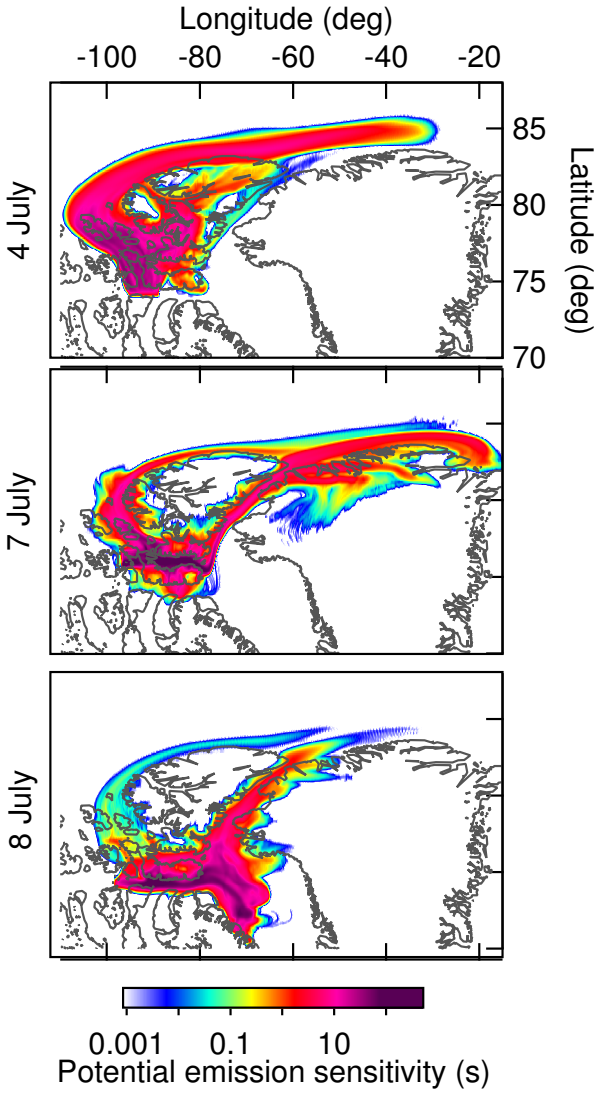

Figure 14. FLEXPART backward simulations of the considered measurement periods (Fig. 12) three days prior to sampling. The color-coded area presents potential emission sensitivity in seconds. Different rows depict different measurement days.

4 Conclusions

We presented results from aircraft-based single particle aerosol measurements in the summertime Canadian High Arctic. Our study has shown the presence of TMA-containing particles in the Arctic summer, comprising 23 % of all analyzed particles (total number of all particles: 7412). We confirmed the identification of TMA marker peaks in single particle mass spectra by laboratory measurements.

Further, we investigated potential emission sources and aerosol chemistry processes of particulate TMA in the summertime Arctic. Observations of an increasing fraction of particulate TMA with decreasing altitude (maximum approximately 60 % in the local BL) suggested the existence of inner-Arctic sources of TMA. Further analysis of wind direction along the flight track and FLEXPART backward simulations demonstrated a marine-biogenic influence on air masses containing particulate TMA. The local oceanic influence on aerosol composition is further evident by the presence of larger (> 600 nm) Na/Cl-containing particles (sea spray particles) in the BL. Some of these sea spray particles were found to be internally mixed with carbohydrates (e.g., cellulose) indicating the existence of a sea surface microlayer enriched with microorganisms and organic compounds. We additionally found that primary sea spray particles and TMA-containing particles are externally mixed although both substances are thought to be released from the ocean. This is one important finding suggesting that TMA acts as a precursor gas for secondary organic aerosol in the Arctic BL. We further conclude that gas-phase TMA, after the release by the ocean, was taken up by acidic aerosol forming aminium sulfate salts as evident by the concurrent existence of sulfate and TMA in single particle spectra. Moreover, the absence of ammonium on 39 % of particles containing TMA shows that TMA may take part in neutralizing acidic aerosol instead of NH_3. It is further possible that gas-to-particle partitioning of TMA was enhanced in the vicinity of clouds and fog through dissolution of TMA in cloud/fog droplets and subsequent acid-base reactions as earlier reported in Rehbein et al. (2011).

In contrast to the discussed marine inner-Arctic sources for summertime Arctic aerosol, we have indications for long-range transport as a further source for particles. Levoglucosan-containing particles (as biomass-burning marker) showed, compared to TMA-containing particles, a higher fraction at higher altitudes as well as larger particles sizes (maximum in the size distribution at 700-800 nm).

Taken together, these findings extend our knowledge of marine-biogenic influences on secondary aerosol chemical composition in the summertime Canadian Arctic. Future wide-spread and long-term Arctic measurements of atmospheric amines would greatly help to extend our results to other Arctic regions.

Author contributions. Jon Abbatt, Richard Leaitch and Andreas Herber designed the research project. Franziska Köllner, Johannes Schneider, Heiko Bozem, Richard Leaitch, Megan Willis and Julia Burkart carried out the measurements. Amir Aliabadi processed the wind measurements. Thomas Klimach, Frank Helleis and Johannes Schneider re-designed and further developed the ALABAMA for aircraft-based measurements. Franziska Köllner analyzed the data with the help of Johannes Schneider, Peter Hoor, Thomas Klimach and Daniel Kunkel. Franziska Köllner wrote the manuscript. All co-authors commented on the manuscript.

Acknowledgements. The authors thank Kenn Borek Air Ltd., in particular our pilots Kevin Elke and John Bayes, as well as our aircraft maintenance engineer Kevin Riehl. We thank Jim Hodgson and Lake Central Air Services in Muskoka, Jim Watson (Scale Modelbuilders, Inc.), Julia Binder and Martin Gehrmann (Alfred Wegener Institute, AWI) for their support of the integration of the instrumentation in the aircraft. We thank Bob Christensen (University of Toronto), Lukas Kandora, Manuel Sellmann, Christian Konrad and Jens Herrmann (AWI), Desiree Toom, Sangeeta Sharma (ECCC), Kathy Law and Jenny Thomas (LATMOS) for their support before and during the study. We thank the Biogeochemistry department of MPIC for providing the CO instrument and Dieter Scharffe for his support during the preparation phase

of the campaign. We thank the Nunavut Research Institute and the Nunavut Impact Review Board for licensing the study. Logistical support in Resolute Bay was provided by the Polar Continental Shelf Project (PCSP) of Natural Resources Canada under PCSP field project 218-14. Funding for this work was provided by the Natural Sciences and Engineering Research Council of Canada through the NETCARE project of the Climate Change and Atmospheric Research Program, the Alfred Wegener Institute, Environment and Climate Change Canada and the Max Planck Society. Special thanks to the whole NETCARE-team for data exchange, discussions and support.

References

Aliabadi, A. A., Staebler, R. M., and Sharma, S.: Air quality monitoring in communities of the Canadian Arctic during the high shipping season with a focus on local and marine pollution, Atmospheric Chemistry and Physics, 15, 2651–2673, doi:10.5194/acp-15-2651-2015, http://www.atmos-chem-phys.net/15/2651/2015/, 2015.

Aliabadi, A. A., Staebler, R., Liu, M., and Herber, A.: Characterization and Parametrization of Reynolds Stress and Turbulent Heat Flux in the Stably-Stratified Lower Arctic Troposphere Using Aircraft Measurements, Boundary-Layer Meteorology, pp. 1–28, doi:10.1007/s10546-016-0164-7, http://link.springer.com/article/10.1007/s10546-016-0164-7, 2016a.

Aliabadi, A. A., Thomas, J. L., Herber, A. B., Staebler, R. M., Leaitch, W. R., Schulz, H., Law, K. S., Marelle, L., Burkart, J., Willis, M. D., Bozem, H., Hoor, P. M., Köllner, F., Schneider, J., Levasseur, M., and Abbatt, J. P. D.: Ship emissions measurement in the Arctic by plume intercepts of the Canadian Coast Guard icebreaker *Amundsen* from the *Polar 6* aircraft platform, Atmospheric Chemistry and Physics, 16, 7899–7916, doi:10.5194/acp-16-7899-2016, http://www.atmos-chem-phys.net/16/7899/2016/, 2016b.

Almeida, J., Schobesberger, S., Kurten, A., Ortega, I. K., Kupiainen-Maatta, O., Praplan, A. P., Adamov, A., Amorim, A., Bianchi, F., Breitenlechner, M., David, A., Dommen, J., Donahue, N. M., Downard, A., Dunne, E., Duplissy, J., Ehrhart, S., Flagan, R. C., Franchin, A., Guida, R., Hakala, J., Hansel, A., Heinritzi, M., Henschel, H., Jokinen, T., Junninen, H., Kajos, M., Kangasluoma, J., Keskinen, H., Kupc, A., Kurten, T., Kvashin, A. N., Laaksonen, A., Lehtipalo, K., Leiminger, M., Leppa, J., Loukonen, V., Makhmutov, V., Mathot, S., McGrath, M. J., Nieminen, T., Olenius, T., Onnela, A., Petaja, T., Riccobono, F., Riipinen, I., Rissanen, M., Rondo, L., Ruuskanen, T., Santos, F. D., Sarnela, N., Schallhart, S., Schnitzhofer, R., Seinfeld, J. H., Simon, M., Sipila, M., Stozhkov, Y., Stratmann, F., Tome, A., Trostl, J., Tsagkogeorgas, G., Vaattovaara, P., Viisanen, Y., Virtanen, A., Vrtala, A., Wagner, P. E., Weingartner, E., Wex, H., Williamson, C., Wimmer, D., Ye, P., Yli-Juuti, T., Carslaw, K. S., Kulmala, M., Curtius, J., Baltensperger, U., Worsnop, D. R., Vehkamaki, H., and Kirkby, J.: Molecular understanding of sulphuric acid-amine particle nucleation in the atmosphere, Nature, 502, 359 – 363, doi:10.1038/nature12663, 2013.

Andreae, M. O.: Soot Carbon and Excess Fine Potassium: Long-Range Transport of Combustion-Derived Aerosols, Science, 220, 1148–1151, doi:10.1126/science.220.4602.1148, http://science.sciencemag.org/content/220/4602/1148, 1983.

Andreae, M. O. and Merlet, P.: Emission of trace gases and aerosols from biomass burning, Global Biogeochemical Cycles, 15, 955–966, doi:10.1029/2000GB001382, http://dx.doi.org/10.1029/2000GB001382, 2001.

Angelino, S., Suess, D. T., and Prather, K. A.: Formation of Aerosol Particles from Reactions of Secondary and Tertiary Alkylamines: Characterization by Aerosol Time-of-Flight Mass Spectrometry, Environmental Science & Technology, 35(15), 3130–3138, doi:10.1021/es0015444, 2001.

Barrie, L. A.: Arctic air pollution: An overview of current knowledge, Atmospheric Environment, 20, 643–663, doi:10.1016/0004-6981(86)90180-0, 1986.

Barsanti, K. C., McMurry, P. H., and Smith, J. N.: The potential contribution of organic salts to new particle growth, Atmospheric Chemistry and Physics, 9, 2949–2957, doi:10.5194/acp-9-2949-2009, http://www.atmos-chem-phys.net/9/2949/2009/, 2009.

Bergman, T., Laaksonen, A., Korhonen, H., Malila, J., Dunne, E. M., Mielonen, T., Lehtinen, K. E. J., Kühn, T., Arola, A., and Kokkola, H.: Geographical and diurnal features of amine-enhanced boundary layer nucleation, Journal of Geophysical Research: Atmospheres, 120, 9606–9624, doi:10.1002/2015JD023181, http://dx.doi.org/10.1002/2015JD023181, 2015JD023181, 2015.

Blanchard, D. C. and Woodcock, A. H.: THE PRODUCTION, CONCENTRATION, AND VERTICAL DISTRIBUTION OF THE SEA-SALT AEROSOL, Annals of the New York Academy of Sciences, 338, 330–347, doi:10.1111/j.1749-6632.1980.tb17130.x, http://dx.doi.org/10.1111/j.1749-6632.1980.tb17130.x, 1980.

Bond, T. C., Bhardwaj, E., Dong, R., Jogani, R., Jung, S., Roden, C., Streets, D. G., and Trautmann, N. M.: Historical emissions of black and organic carbon aerosol from energy-related combustion, 1850–2000, Global Biogeochemical Cycles, 21, n/a–n/a, doi:10.1029/2006GB002840, http://dx.doi.org/10.1029/2006GB002840, gB2018, 2007.

Brands, M., Kamphus, M., Böttger, T., Schneider, J., Drewnick, F., Roth, A., Curtius, J., Voigt, C., Borbon, A., Beekmann, M., Bourdon, A., Perrin, T., and Borrmann, S.: Characterization of a Newly Developed Aircraft-Based Laser Ablation Aerosol Mass Spectrometer (ALABAMA) and First Field Deployment in Urban Pollution Plumes over Paris During MEGAPOLI 2009, Aerosol Science and Technology, 45, 46–64, doi:10.1080/02786826.2010.517813, http://dx.doi.org/10.1080/02786826.2010.517813, 2011.

Burkart, J., Willis, M. D., Bozem, H., Thomas, J. L., Law, K., Hoor, P., Aliabadi, A. A., Köllner, F., Schneider, J., Herber, A., Abbatt, J. P. D., and Leaitch, W. R.: Summertime observations of elevated levels of ultrafine particles in the high Arctic marine boundary layer, Atmospheric Chemistry and Physics, 17, 5515–5535, doi:10.5194/acp-17-5515-2017, http://www.atmos-chem-phys.net/17/5515/2017/, 2017.

Chapman, W. L. and Walsh, J. E.: Recent Variations of Sea Ice and Air Temperature in High Latitudes, Bulletin of the American Meteorological Society, 74, 33–47, doi:10.1175/1520-0477(1993)074<0033:RVOSIA>2.0.CO;2, http://dx.doi.org/10.1175/1520-0477(1993)074<0033:RVOSIA>2.0.CO;2, 1993.

Corbin, J., Rehbein, P., Evans, G., and Abbatt, J.: Combustion particles as ice nuclei in an urban environment: Evidence from single-particle mass spectrometry., Atmospheric Environment, 51, 286(7), 2012.

Croft, B., Martin, R. V., Leaitch, W. R., Tunved, P., Breider, T. J., D'Andrea, S. D., and Pierce, J. R.: Processes controlling the annual cycle of Arctic aerosol number and size distributions, Atmospheric Chemistry and Physics, 16, 3665–3682, doi:10.5194/acp-16-3665-2016, http://www.atmos-chem-phys.net/16/3665/2016/, 2016a.

Croft, B., Wentworth, G. R., Martin, R. V., Leaitch, W. R., Murphy, J. G., Murphy, B. N., Kodros, J. K., and AU Abbatt, J. P. D. AU Pierce, J. R.: Contribution of Arctic seabird-colony ammonia to atmospheric particles and cloud-albedo radiative effect, Nature Communications, 7, doi:10.1038/ncomms13444, 2016b.

Dall'Osto, M., Ceburnis, D., Monahan, C., Worsnop, D. R., Bialek, J., Kulmala, M., Kurtén, T., Ehn, M., Wenger, J., Sodeau, J., Healy, R., and O'Dowd, C.: Nitrogenated and aliphatic organic vapors as possible drivers for marine secondary organic aerosol growth, Journal of Geophysical Research: Atmospheres, 117, n/a–n/a, doi:10.1029/2012JD017522, http://dx.doi.org/10.1029/2012JD017522, d12311, 2012.

Dawson, M. L., Varner, M. E., Perraud, V., Ezell, M. J., Gerber, R. B., and Finlayson-Pitts, B. J.: Simplified mechanism for new particle formation from methanesulfonic acid, amines, and water via experiments and ab initio calculations, Proceedings of the National Academy of Sciences, 109, 18 719–18 724, doi:10.1073/pnas.1211878109, http://www.pnas.org/content/109/46/18719.abstract, 2012.

Engvall, A.-C., Krejci, R., Ström, J., Treffeisen, R., Scheele, R., Hermansen, O., and Paatero, J.: Changes in aerosol properties during spring-summer period in the Arctic troposphere, Atmospheric Chemistry and Physics, 8, 445–462, doi:10.5194/acp-8-445-2008, http://www.atmos-chem-phys.net/8/445/2008/, 2008.

Erupe, M. E., Viggiano, A. A., and Lee, S.-H.: The effect of trimethylamine on atmospheric nucleation involving H_2SO_4, Atmospheric Chemistry and Physics, 11, 4767–4775, doi:10.5194/acp-11-4767-2011, http://www.atmos-chem-phys.net/11/4767/2011/, 2011.

Facchini, M. C., Decesari, S., Rinaldi, M., Carbone, C., Finessi, E., Mircea, M., Fuzzi, S., Moretti, F., Tagliavini, E., Ceburnis, D., and O'Dowd, C. D.: Important Source of Marine Secondary Organic Aerosol from Biogenic Amines, Environmental Science & Technology, 42, 9116–9121, doi:10.1021/es8018385, http://dx.doi.org/10.1021/es8018385, pMID: 19174880, 2008.

Frossard, A. A., Russell, L. M., Burrows, S. M., Elliott, S. M., Bates, T. S., and Quinn, P. K.: Sources and composition of submicron organic mass in marine aerosol particles, Journal of Geophysical Research: Atmospheres, 119, 12,977–13,003, doi:10.1002/2014JD021913, http://dx.doi.org/10.1002/2014JD021913, 2014JD021913, 2014.

Gaston, C. J., Pratt, K. A., Qin, X., and Prather, K. A.: Real-Time Detection and Mixing State of Methanesulfonate in Single Particles at an Inland Urban Locaion during a Phytoplankton Bloom, Environmental Science & Technology, 44(5), 1566–1572, doi:10.1021/es902069d, 2010.

Ge, X., Wexler, A. S., and Clegg, S. L.: Atmospheric amines - Part I. A review, Atmospheric Environment, 45, 524 – 546, doi:http://dx.doi.org/10.1016/j.atmosenv.2010.10.012, http://www.sciencedirect.com/science/article/pii/S1352231010008745, 2011a.

Ge, X., Wexler, A. S., and Clegg, S. L.: Atmospheric amines - Part II. Thermodynamic properties and gas/particle partitioning, Atmospheric Environment, 45, 561 – 577, doi:http://dx.doi.org/10.1016/j.atmosenv.2010.10.013, http://www.sciencedirect.com/science/article/pii/S1352231010008757, 2011b.

Gibb, S. W., Mantoura, R. F. C., and Liss, P. S.: Ocean-atmosphere exchange and atmospheric speciation of ammonia and methylamines in the region of the NW Arabian Sea, Global Biogeochemical Cycles, 13, 161–178, doi:10.1029/98GB00743, http://dx.doi.org/10.1029/98GB00743, 1999.

Glasoe, W. A., Volz, K., Panta, B., Freshour, N., Bachman, R., Hanson, D. R., McMurry, P. H., and Jen, C.: Sulfuric acid nucleation: An experimental study of the effect of seven bases, Journal of Geophysical Research: Atmospheres, 120, 1933–1950, doi:10.1002/2014JD022730, http://dx.doi.org/10.1002/2014JD022730, 2014JD022730, 2015.

Hawkins, L. N. and Russell, L. M.: Polysaccharides, Proteins, and Phytoplankton Fragments: Four Chemically Distinct Types of Marine Primary Organic Aerosol Classified by Single Particle Spectromicroscopy, Advances in Meteorology, 2010, 14 pages, doi:10.1155/2010/612132, 2010.

Haywood, J. and Boucher, O.: Estimates of the direct and indirect radiative forcing due to tropospheric aerosols: A review, Reviews of Geophysics, 38, 513–543, doi:10.1029/1999RG000078, http://dx.doi.org/10.1029/1999RG000078, 2000.

Healy, R. M., Evans, G. J., Murphy, M., Sierau, B., Arndt, J., McGillicuddy, E., O'Connor, I. P., Sodeau, J. R., and Wenger, J. C.: Single-particle speciation of alkylamines in ambient aerosol at five European sites, Analytical and Bioanalytical Chemistry, 407, 5899–5909, doi:10.1007/s00216-014-8092-1, http://dx.doi.org/10.1007/s00216-014-8092-1, 2015.

Heintzenberg, J., Tunved, P., Galí, M., and Leck, C.: New particle formation in the Svalbard region 2006–2015, Atmospheric Chemistry and Physics, 17, 6153–6175, doi:10.5194/acp-17-6153-2017, http://www.atmos-chem-phys.net/17/6153/2017/, 2017.

Herber, A. B., Dethloff, K., Haas, C., Steinhage, D., Strapp, J. W., Bottenheim, J., McElroy, T., and Yamanouchi, T.: POLAR 5 - a new research aircraft for improved access to the Arctic, ISAR-1, Drastic Change under the Global Warming, Extended Abstract, 2008.

IPCC, .: Climate Change 2014: Synthesis Report. Contribution of Working Groups I, II and III to the Fifth Assessment Report of the Intergovernmental Panel on Climate Change [Core Writing Team, R.K. Pachauri and L.A. Meyer (eds.)]. IPCC, Geneva, Switzerland, 151 pp., 2014.

Jen, C. N., McMurry, P. H., and Hanson, D. R.: Stabilization of sulfuric acid dimers by ammonia, methylamine, dimethylamine, and trimethylamine, Journal of Geophysical Research: Atmospheres, 119, 7502–7514, doi:10.1002/2014JD021592, http://dx.doi.org/10.1002/2014JD021592, 2014JD021592, 2014.

Jen, C. N., Bachman, R., Zhao, J., McMurry, P. H., and Hanson, D. R.: Diamine-sulfuric acid reactions are a potent source of new particle formation, Geophysical Research Letters, pp. n/a–n/a, doi:10.1002/2015GL066958, http://dx.doi.org/10.1002/2015GL066958, 2015GL066958, 2016.

Kawamura, K., Kasukabe, H., and Barrie, L. A.: Source and reaction pathways of dicarboxylic acids, ketoacids and dicarbonyls in arctic aerosols: One year of observations, Atmospheric Environment, 30, 1709 – 1722, doi:http://dx.doi.org/10.1016/1352-2310(95)00395-9, http://www.sciencedirect.com/science/article/pii/1352231095003959, 1996.

Kawamura, K., Kasukabe, H., and Barrie, L. A.: Secondary formation of water-soluble organic acids and α-dicarbonyls and their contributions to total carbon and water-soluble organic carbon: Photochemical aging of organic aerosols in the Arctic spring, Journal of Geophysical Research: Atmospheres, 115, n/a–n/a, doi:10.1029/2010JD014299, http://dx.doi.org/10.1029/2010JD014299, d21306, 2010.

Klimach, T.: Chemische Zusammensetzung der Aerosole: Design und Datenauswertung eines Einzelpartikel-Laserablationsmassenspektrometers, Ph.D. thesis, Johannes-Gutenberg Universität Mainz, 2012.

Kupiszewski, P., Leck, C., Tjernström, M., Sjogren, S., Sedlar, J., Graus, M., Müller, M., Brooks, B., Swietlicki, E., Norris, S., and Hansel, A.: Vertical profiling of aerosol particles and trace gases over the central Arctic Ocean during summer, Atmospheric Chemistry and Physics, 13, 12 405–12 431, doi:10.5194/acp-13-12405-2013, http://www.atmos-chem-phys.net/13/12405/2013/, 2013.

Lakshmanan, C. M., Gal-or, B., and Hoelscher, H. E.: Production of Levoglucosan by Pyrolysis of Carbohydrates, Product R&D, 8, 261–267, doi:10.1021/i360031a010, http://dx.doi.org/10.1021/i360031a010, 1969.

Law, K. S. and Stohl, A.: Arctic Air Pollution: Origins and Impacts, Science, 315, 1537–1540, doi:10.1126/science.1137695, http://science.sciencemag.org/content/315/5818/1537, 2007.

Leaitch, W. R., Sharma, S., Huang, L., Toom-Sauntry, D., Chivulescu, A., Macdonald, A. M., von Salzen, K., Pierce, J. R., Bertram, A. K., Schroder, J. C., Shantz, N. C., Chang, R. Y.-W., and Norman, A.-L.: Dimethyl sulfide control of the clean summertime Arctic aerosol and cloud, Elementa: Science of the Anthropocene, doi:DOI 10.12952/journal.elementa.000017, http://elementascience.org/article/info%3Adoi%2F10.12952%2Fjournal.elementa.000017, 2013.

Leaitch, W. R., Korolev, A., Aliabadi, A. A., Burkart, J., Willis, M. D., Abbatt, J. P. D., Bozem, H., Hoor, P., Köllner, F., Schneider, J., Herber, A., Konrad, C., and Brauner, R.: Effects of 20–100 nm particles on liquid clouds in the clean summertime Arctic, Atmospheric Chemistry and Physics, 16, 11 107–11 124, doi:10.5194/acp-16-11107-2016, http://www.atmos-chem-phys.net/16/11107/2016/, 2016.

Li, J., Pósfai, M., Hobbs, P. V., and Buseck, P. R.: Individual aerosol particles from biomass burning in southern Africa: 2, Compositions and aging of inorganic particles, Journal of Geophysical Research: Atmospheres, 108, n/a–n/a, doi:10.1029/2002JD002310, http://dx.doi.org/10.1029/2002JD002310, 8484, 2003.

Li, Q., Jacob, D. J., Bey, I., Yantosca, R. M., Zhao, Y., Kondo, Y., and Notholt, J.: Atmospheric hydrogen cyanide (HCN): Biomass burning source, ocean sink?, Geophysical Research Letters, 27, 357–360, doi:10.1029/1999GL010935, http://dx.doi.org/10.1029/1999GL010935, 2000.

Liu, P., Ziemann, P. J., Kittelson, D. B., and McMurry, P. H.: Generating Particle Beams of Controlled Dimensions and Divergence: I. Theory of Particle Motion in Aerodynamic Lenses and Nozzle Expansions, Aerosol Science and Technology, 22, 293–313, doi:10.1080/02786829408959748, http://dx.doi.org/10.1080/02786829408959748, 1995a.

Liu, P., Ziemann, P. J., Kittelson, D. B., and McMurry, P. H.: Generating Particle Beams of Controlled Dimensions and Divergence: II. Experimental Evaluation of Particle Motion in Aerodynamic Lenses and Nozzle Expansions, Aerosol Science and Technology, 22, 314–324, doi:10.1080/02786829408959749, http://dx.doi.org/10.1080/02786829408959749, 1995b.

Müller, C., Iinuma, Y., Karstensen, J., van Pinxteren, D., Lehmann, S., Gnauk, T., and Herrmann, H.: Seasonal variation of aliphatic amines in marine sub-micrometer particles at the Cape Verde islands, Atmospheric Chemistry and Physics, 9, 9587–9597, doi:10.5194/acp-9-9587-2009, http://www.atmos-chem-phys.net/9/9587/2009/, 2009.

Mungall, E. L., Croft, B., Lizotte, M., Thomas, J. L., Murphy, J. G., Levasseur, M., Martin, R. V., Wentzell, J. J. B., Liggio, J., and Abbatt, J. P. D.: Dimethyl sulfide in the summertime Arctic atmosphere: measurements and source sensitivity simulations, Atmospheric Chemistry and Physics, 16, 6665–6680, doi:10.5194/acp-16-6665-2016, http://www.atmos-chem-phys.net/16/6665/2016/, 2016.

Murphy, S. M., Sorooshian, A., Kroll, J. H., Ng, N. L., Chhabra, P., Tong, C., Surratt, J. D., Knipping, E., Flagan, R. C., and Seinfeld, J. H.: Secondary aerosol formation from atmospheric reactions of aliphatic amines, Atmospheric Chemistry and Physics, 7, 2313–2337, doi:10.5194/acp-7-2313-2007, http://www.atmos-chem-phys.net/7/2313/2007/, 2007.

Neubauer, K. R., Johnston, M. V., and Wexler, A. S.: Humidity effects on the mass spectra of single aerosol particles, Atmospheric Environment, 32, 2521–2529, 1998.

O'Dowd, C. D. and de Leeuw, G.: Marine aerosol production: a review of the current knowledge, Phil. Trans. R. Soc. A, 365, 1753–1774, doi:10.1098/rsta.2007.2043, 2007.

O'Dowd, C. D., Lowe, J. A., and Smith, M. H.: Coupling sea-salt and sulphate interactions and its impact on cloud droplet concentration predictions, Geophysical Research Letters, 26, 1311–1314, doi:10.1029/1999GL900231, http://dx.doi.org/10.1029/1999GL900231, 1999.

Pankow, J. F.: Phase considerations in the gas/particle partitioning of organic amines in the atmosphere, Atmospheric Environment, 122, 448 – 453, doi:http://dx.doi.org/10.1016/j.atmosenv.2015.09.056, http://www.sciencedirect.com/science/article/pii/S1352231015303988, 2015.

Pöhlker, C., Wiedemann, K. T., Sinha, B., Shiraiwa, M., Gunthe, S. S., Smith, M., Su, H., Artaxo, P., Chen, Q., Cheng, Y., Elbert, W., Gilles, M. K., Kilcoyne, A. L. D., Moffet, R. C., Weigand, M., Martin, S. T., Pöschl, U., and Andreae, M. O.: Biogenic Potassium Salt Particles as Seeds for Secondary Organic Aerosol in the Amazon, Science, 337, 1075, doi:10.1126/science.1223264, 2012.

Pratt, K. A., Hatch, L. E., and Prather, K. A.: Seasonal Volatility Dependence of Ambient Particle Phase Amines, Environmental Science & Technology, 43 (14), 5276–5281, doi:10.1021/es803189n, 2009.

Quinn, P. K., Shaw, G., Andrews, E., Dutton, E. G., Ruoho-Airola, T., and Gong, S. L.: Arctic haze: current trends and knowledge gaps, Tellus B, 59, 99–114, doi:10.1111/j.1600-0889.2006.00238.x, http://dx.doi.org/10.1111/j.1600-0889.2006.00238.x, 2007.

Quinn, P. K., Bates, T. S., Schulz, K. S., Coffman, D. J., Frossard, A. A., Russell, L. M., Keene, W. C., and Kieber, D. J.: Contribution of sea surface carbon pool to organic matter enrichment in sea spray aerosol, Nature Geosci, 7, 228–232, doi:10.1038/ngeo2092, 2014.

Rahn, K. A. and McCaffrey, R. J.: ON THE ORIGIN AND TRANSPORT OF THE WINTER ARCTIC AEROSOL, Annals of the New York Academy of Sciences, 338, 486–503, doi:10.1111/j.1749-6632.1980.tb17142.x, http://dx.doi.org/10.1111/j.1749-6632.1980.tb17142.x, 1980.

Rehbein, P. J. G., Jeong, C.-H., McGuire, M. L., Yao, X., Corbin, J. C., and Evans, G. J.: Cloud and Fog Processing Enhanced Gas-to-Particle Partitioning of Trimethylamine, Environmental Science & Technology, 45, 4346–4352, doi:10.1021/es1042113, http://dx.doi.org/10.1021/es1042113, pMID: 21488635, 2011.

Roth, A., Schneider, J., Klimach, T., Mertes, S., van Pinxteren, D., Herrmann, H., and Borrmann, S.: Aerosol properties, source identification, and cloud processing in orographic clouds measured by single particle mass spectrometry on a central European mountain site during HCCT-2010, Atmospheric Chemistry and Physics, 16, 505–524, doi:10.5194/acp-16-505-2016, http://www.atmos-chem-phys.net/16/505/2016/, 2016.

Salter, M. E., Hamacher-Barth, E., Leck, C., Werner, J., Johnson, C. M., Riipinen, I., Nilsson, E. D., and Zieger, P.: Calcium enrichment in sea spray aerosol particles, Geophysical Research Letters, 43, 8277–8285, doi:10.1002/2016GL070275, http://dx.doi.org/10.1002/2016GL070275, 2016GL070275, 2016.

Scalabrin, E., Zangrando, R., Barbaro, E., Kehrwald, N. M., Gabrieli, J., Barbante, C., and Gambaro, A.: Amino acids in Arctic aerosols, Atmospheric Chemistry and Physics, 12, 10 453–10 463, doi:10.5194/acp-12-10453-2012, http://www.atmos-chem-phys.net/12/10453/2012/, 2012.

Schmale, J., Schneider, J., Ancellet, G., Quennehen, B., Stohl, A., Sodemann, H., Burkhart, J. F., Hamburger, T., Arnold, S. R., Schwarzenboeck, A., Borrmann, S., and Law, K. S.: Source identification and airborne chemical characterisation of aerosol pollution from long-range transport over Greenland during POLARCAT summer campaign 2008, Atmospheric Chemistry and Physics, 11, 10 097–10 123, doi:10.5194/acp-11-10097-2011, http://www.atmos-chem-phys.net/11/10097/2011/, 2011.

Schmale, J., Schneider, J., Nemitz, E., Tang, Y. S., Dragosits, U., Blackall, T. D., Trathan, P. N., Phillips, G. J., Sutton, M., and Braban, C. F.: Sub-Antarctic marine aerosol: dominant contributions from biogenic sources, Atmospheric Chemistry and Physics, 13, 8669–8694, doi:10.5194/acp-13-8669-2013, http://www.atmos-chem-phys.net/13/8669/2013/, 2013.

Schmidt, S., Schneider, J., Klimach, T., Mertes, S., Schenk, L. P., Kupiszewski, P., Curtius, J., and Borrmann, S.: Online single particle analysis of ice particle residuals from mountain-top mixed-phase clouds using laboratory derived particle type assignment, Atmospheric Chemistry and Physics, 17, 575–594, doi:10.5194/acp-17-575-2017, http://www.atmos-chem-phys.net/17/575/2017/, 2017.

Serreze, M. C., Barrett, A. P., Stroeve, J. C., Kindig, D. N., and Holland, M. M.: The emergence of surface-based Arctic amplification, The Cryosphere, 3, 11–19, doi:10.5194/tc-3-11-2009, http://www.the-cryosphere.net/3/11/2009/, 2009.

Sharma, S., Chan, E., Ishizawa, M., Toom-Sauntry, D., Gong, S. L., Li, S. M., Tarasick, D. W., Leaitch, W. R., Norman, A., Quinn, P. K., Bates, T. S., Levasseur, M., Barrie, L. A., and Maenhaut, W.: Influence of transport and ocean ice extent on biogenic aerosol sulfur in the Arctic atmosphere, Journal of Geophysical Research: Atmospheres, 117, n/a–n/a, doi:10.1029/2011JD017074, http://dx.doi.org/10.1029/2011JD017074, d12209, 2012.

Sierau, B., Chang, R. Y.-W., Leck, C., Paatero, J., and Lohmann, U.: Single-particle characterization of the high-Arctic summertime aerosol, Atmospheric Chemistry and Physics, 14, 7409–7430, doi:10.5194/acp-14-7409-2014, http://www.atmos-chem-phys.net/14/7409/2014/, 2014.

Silva, P. J., Liu, D.-Y., Noble, C. A., and Prather, K. A.: Size and Chemical Characterization of Individual Particles Resulting from Biomass Burning of Local Southern California Species, Environmental Science & Technology, 33, 3068–3076, doi:10.1021/es980544p, http://dx.doi.org/10.1021/es980544p, 1999.

Simoneit, B., Schauer, J., Nolte, C., Oros, D., Elias, V., Fraser, M., Rogge, W., and Cass, G.: Levoglucosan, a tracer for cellulose in biomass burning and atmospheric particles, Atmospheric Environment, 33, 173–182, 1999.

Simoneit, B. R.: Biomass burning - review of organic tracers for smoke from incomplete combustion, Applied Geochemistry, 17, 129 – 162, doi:http://dx.doi.org/10.1016/S0883-2927(01)00061-0, http://www.sciencedirect.com/science/article/pii/S0883292701000610, 2002.

Smith, J. N., Barsanti, K. C., Friedli, H. R., Ehn, M., Kulmala, M., Collins, D. R., Scheckman, J. H., Williams, B. J., and McMurry, P. H.: Observations of aminium salts in atmospheric nanoparticles and possible climatic implications, Proceedings of the National Academy of Sciences, 107, 6634–6639, doi:10.1073/pnas.0912127107, http://www.pnas.org/content/107/15/6634.abstract, 2010.

Sorensen, L. L., Pryor, S. C., de Leeuw, G., and Schulz, M.: Flux divergence of nitric acid in the marine atmospheric surface layer, Journal of Geophysical Research: Atmospheres, 110, n/a–n/a, doi:10.1029/2004JD005403, http://dx.doi.org/10.1029/2004JD005403, d15306, 2005.

Stohl, A.: Characteristics of atmospheric transport into the Arctic troposphere, Journal of Geophysical Research: Atmospheres, 111, n/a–n/a, doi:10.1029/2005JD006888, http://dx.doi.org/10.1029/2005JD006888, d11306, 2006.

Stohl, A., Forster, C., Frank, A., Seibert, P., and Wotawa, G.: Technical note: The Lagrangian particle dispersion model FLEXPART version 6.2, Atmospheric Chemistry and Physics, 5, 2461–2474, doi:10.5194/acp-5-2461-2005, http://www.atmos-chem-phys.net/5/2461/2005/, 2005.

Tunved, P., Ström, J., and Krejci, R.: Arctic aerosol life cycle: linking aerosol size distributions observed between 2000 and 2010 with air mass transport and precipitation at Zeppelin station, Ny-Ålesund, Svalbard, Atmospheric Chemistry and Physics, 13, 3643–3660, doi:10.5194/acp-13-3643-2013, http://www.atmos-chem-phys.net/13/3643/2013/, 2013.

Van Neste, A., Duce, R. A., and Lee, C.: Methylamines in the marine atmosphere, Geophysical Research Letters, 14, 711–714, doi:10.1029/GL014i007p00711, http://dx.doi.org/10.1029/GL014i007p00711, 1987.

Wentworth, G. R., Murphy, J. G., Croft, B., Martin, R. V., Pierce, J. R., Côté, J.-S., Courchesne, I., Tremblay, J.-E., Gagnon, J., Thomas, J. L., Sharma, S., Toom-Sauntry, D., Chivulescu, A., Levasseur, M., and Abbatt, J. P. D.: Ammonia in the summertime Arctic marine boundary layer: sources, sinks, and implications, Atmospheric Chemistry and Physics, 16, 1937–1953, doi:10.5194/acp-16-1937-2016, http://www.atmos-chem-phys.net/16/1937/2016/, 2016.

Willis, M. D., Burkart, J., Thomas, J. L., Köllner, F., Schneider, J., Bozem, H., Hoor, P. M., Aliabadi, A. A., Schulz, H., Herber, A. B., Leaitch, W. R., and Abbatt, J. P. D.: Growth of nucleation mode particles in the summertime Arctic: a case study, Atmospheric Chemistry and Physics, 16, 7663–7679, doi:10.5194/acp-16-7663-2016, http://www.atmos-chem-phys.net/16/7663/2016/, 2016.

Wilson, T. W., Ladino, L. A., Alpert, P. A., Breckels, M. N. B., Brooks, I. M., Browse, J., Burrows, S. M., Carslaw, K. S., Huffman, J. A., Judd, C., Kilthau, W. P., Mason, R. H., McFiggans, G., Miller, L. A., Nájera, J. J., Polishchuk, E., Rae, S., Schiller, C. L., Si, M., Temprado, J. V., Whale, T. F., Wong, J. P. S., Wurl, O., Jakobi-Hancock, J. D. Y., Abbatt, J. P. D., Aller, J. Y., Bertram, A. K., Knopf, D. A. K., and Murray, B. J.: A marine biogenic source of atmospheric ice-nucleating particles, Nature, 525, 234 – 238, doi:10.1038/nature14986, 2015.

You, Y., Kanawade, V. P., de Gouw, J. A., Guenther, A. B., Madronich, S., Sierra-Hernández, M. R., Lawler, M., Smith, J. N., Takahama, S., Ruggeri, G., Koss, A., Olson, K., Baumann, K., Weber, R. J., Nenes, A., Guo, H., Edgerton, E. S., Porcelli, L., Brune, W. H., Goldstein, A. H., and Lee, S.-H.: Atmospheric amines and ammonia measured with a chemical ionization mass spectrometer (CIMS), Atmospheric Chemistry and Physics, 14, 12 181–12 194, doi:10.5194/acp-14-12181-2014, http://www.atmos-chem-phys.net/14/12181/2014/, 2014.

Youn, J.-S., Crosbie, E., Maudlin, L., Wang, Z., and Sorooshian, A.: Dimethylamine as a major alkyl amine species in particles and cloud water: Observations in semi-arid and coastal regions, Atmospheric Environment, 122, 250 – 258, doi:http://dx.doi.org/10.1016/j.atmosenv.2015.09.061, http://www.sciencedirect.com/science/article/pii/S1352231015304039, 2015.

Yu, H., McGraw, R., and Lee, S.-H.: Effects of amines on formation of sub-3 nm particles and their subsequent growth, Geophysical Research Letters, 39, n/a–n/a, doi:10.1029/2011GL050099, http://dx.doi.org/10.1029/2011GL050099, l02807, 2012.